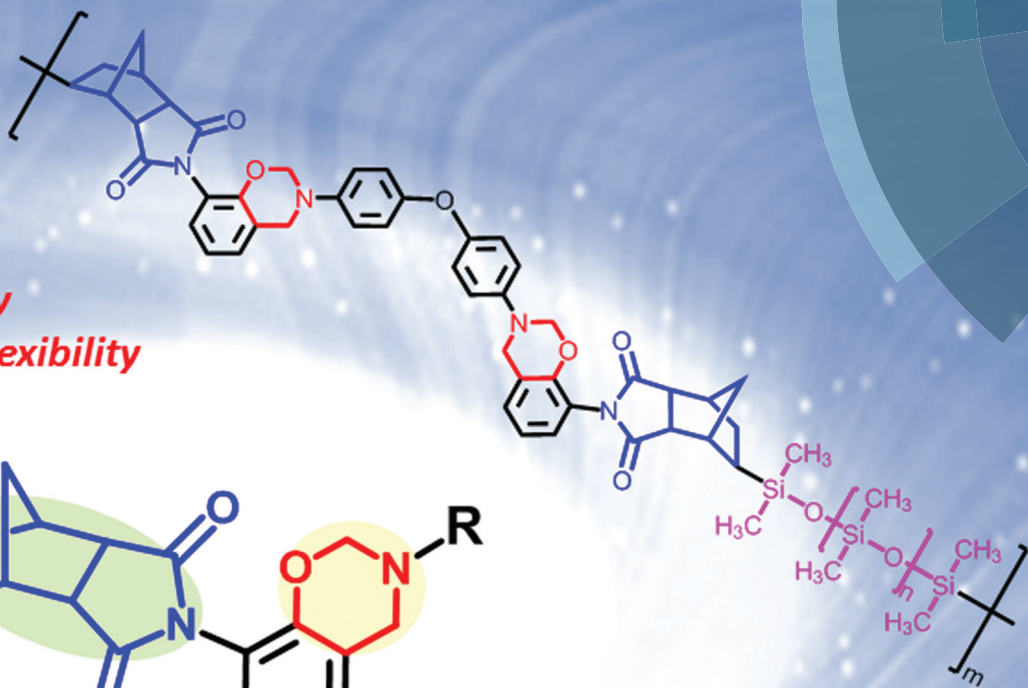


Polymer Chemistry

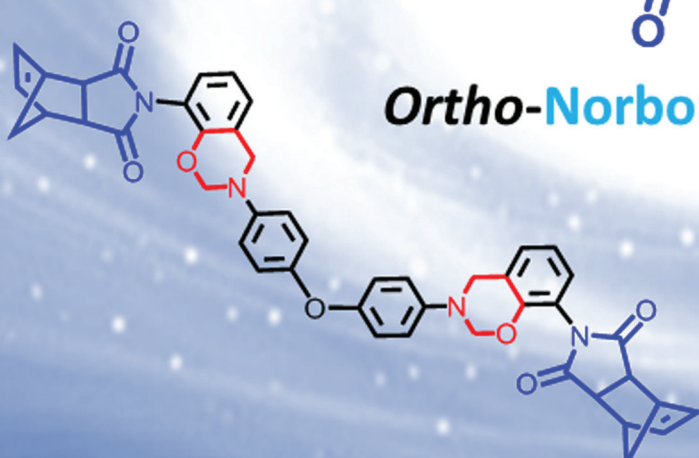
rsc.li/polymers



Easy synthesis
Easy Processability
High Thermal Stability
Excellent molecular design flexibility



Ortho-Norbornene Benzoxazine



ISSN 1759-9962

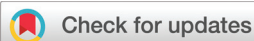


ROYAL SOCIETY
OF CHEMISTRY

Celebrating
IYPT 2019

PAPER

Kan Zhang, Shiao-Wei Kuo *et al.*
Outstanding dielectric and thermal properties of main
chain-type poly(benzoxazine-co-imide-co-siloxane)-based
cross-linked networks



Cite this: *Polym. Chem.*, 2019, **10**, 2387

Outstanding dielectric and thermal properties of main chain-type poly(benzoxazine-co-imide-co-siloxane)-based cross-linked networks†

Kan Zhang,  *^a Xinye Yu^a and Shiao-Wei Kuo  *^{b,c}

In this study we used a facile approach to synthesize poly(benzoxazine-co-imide-co-siloxane) (oHPNI-oda-PDMS), a new main chain-type copolymer featuring benzoxazine, imide, and siloxane units as repeating units. In contrast to previously reported polydimethylsiloxane (PDMS)-containing benzoxazine resins, oHPNI-oda-PDMS was formed directly through hydrosilylation of an *ortho*-norbornene functionalized bisbenzoxazine monomer (oHPNI-oda) and PDMS. Nuclear magnetic resonance and Fourier transform infrared (FTIR) spectroscopy confirmed the chemical structures of oHPNI-oda and oHPNI-oda-PDMS. We used differential scanning calorimetry and *in situ* FTIR spectroscopy to investigate the polymerization behavior of both the benzoxazine monomer and the copolymer, and used dynamic mechanical analysis, thermogravimetric analysis, and microscale combustion calorimetry to determine the thermal properties and flame retardancy of the cross-linked polybenzoxazines. The polybenzoxazine derived from oHPNI-oda-PDMS possessed an excellent combination of properties—high thermal stability, low flammability, and very low dielectric constants ($k = 2.36\text{--}2.29$)—suggesting many potential applications in aerospace, microelectronics, and flame-resistant materials.

Received 27th March 2019,
Accepted 18th April 2019

DOI: 10.1039/c9py00464e

rsc.li/polymers

Introduction

Polybenzoxazines are relatively new, yet fully established, thermosetting resins that have been investigated extensively for a couple of decades because of their potentially useful properties, including high glass transition temperatures,^{1,2} very high char yields,³ excellent physical and mechanical properties,⁴ low humidity uptake,⁵ negligible volumetric shrinkage,⁶ and minimal byproduct formation during polymerization.^{7,8} Another special characteristic of polybenzoxazines is their highly flexible molecular design, more so than any other polymeric material.^{9–12} Furthermore, polybenzoxazines can be obtained readily through thermally activated polymerization of 1,3-benzoxazines, with or without an added catalyst and/or an initiator.¹³ Notably, no alkaline catalysts or strong acids are required during the synthesis of benzoxazine resins. Most benzoxazine-related

investigations have focused on the preparation of polybenzoxazines from precursor monomers. From syntheses based on the traditional benzoxazine monomer, brittleness and difficulty in processing the polymers into thin films have limited their applications and remain problems to be solved.

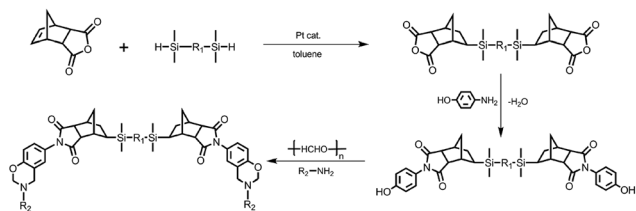
Some recent activities in the benzoxazine field have been concerned with replacing the mono-functional phenols or amines with di-functional species and, thereby, achieve benzoxazines of higher molecular weights. Replacing either the amines or phenols leads to benzoxazine molecules featuring two oxazine rings, which could possibly increase the cross-linking density of the resulting polybenzoxazines. In addition, main chain-type linear polymeric precursors, featuring a benzoxazine monomer as the repeating unit in the main chain, can be obtained when starting from both di-functional amines and phenols.^{14–17} Several strategies have been developed to improve the toughness, as well as the mechanical and thermal properties, of main chain-type polybenzoxazines.^{2,14,18–21} For example, Kiskan *et al.* reported a method for synthesizing oligosiloxanes with benzoxazine functionalities in the main chain *via* Pt-catalyzed hydrosilylation between the tetramethyldisiloxane and diallylbisbenzoxazines.²¹ The thermosets derived from the main chain-type benzoxazine-containing oligosiloxanes exhibited high thermal stability, due to the existence of siloxane units in the polybenzoxazine networks.²¹ Moreover, a series of siloxane-imide-containing benzoxazines have been pre-

^aResearch School of Polymeric Materials, School of Materials Science and Engineering, Jiangsu University, Zhenjiang 212013, China.
E-mail: zhangkan@ujs.edu.cn

^bDepartment of Materials and Optoelectronic Science, Center of Crystal Research, National Sun Yat-Sen University, Kaohsiung, 804, Taiwan.
E-mail: kuosw@faculty.nsysu.edu.tw

^cDepartment of Medicinal and Applied Chemistry, Kaohsiung Medical University, Kaohsiung, 807, Taiwan

†Electronic supplementary information (ESI) available. See DOI: 10.1039/c9py00464e



Scheme 1 Previously reported methods for preparing siloxane-imide-containing benzoxazine resins.

pared using hydrosilylation, as indicated in Scheme 1.^{22–24} The polybenzoxazines based on these siloxane-imide-containing benzoxazines have displayed excellent thermal stabilities and low surface free energies.^{22–24} Nevertheless, the path followed to prepare the siloxane-imide-containing benzoxazines required multiple reactions, and only oligomers with two oxazine rings as terminal groups could be obtained.

Benzoxazine monomers derived from *ortho*-substituted phenols have significant advantages over their *para*-counterparts in terms of the synthesis conditions, the polymerization temperatures, and the thermal, mechanical, and dielectric properties of the resulting polymers.^{25–30} Among these benzoxazines, *ortho*-norbornene-functionalized benzoxazines have an additional possible polymerization mechanism, other than the general ring-opening polymerization of the oxazine rings.^{27,28} Furthermore, *ortho*-norbornene-functionalized bisbenzoxazine monomers can be synthesized readily through Mannich condensation.²⁷

By combining the thermoplastic characteristics of polydimethylsiloxane (PDMS) and the thermosetting nature of *ortho*-norbornene-functional bisbenzoxazines, in this study we prepared a novel main chain-type copolymer featuring benzoxazine, imide, and siloxane functionalities as repeating units, herein termed poly(benzoxazine-*co*-imide-*co*-siloxane) (*o*HPNI-*oda*-PDMS). Compared with other traditional polybenzoxazine resins, this new polybenzoxazine displays higher thermal stability, lower flammability, and a lower dielectric constant.⁹ This paper describes the synthesis and polymerization behavior of the benzoxazine resin, as well as the thermal and mechanical properties of this resulting polybenzoxazine.

Experimental

Materials

endo-5-Norbornene-2,3-dicarboxylic anhydride, paraformaldehyde (99%), sodium hydroxide (NaOH), *o*-aminophenol (99%), toluene, hexanes, and magnesium sulfate were obtained from Sahn Chemical Technology (China) and used as received. 4,4'-Oxydianiline (*oda*), platinum divinyltetramethyldisiloxane complex [Pt(dvs)], and hydride-terminated PDMS ($M_n = 580 \text{ g mol}^{-1}$) were purchased from Energy Reagent (China). The *o*HPNI was prepared as described previously.^{27,28}

Characterization

Nuclear magnetic resonance (NMR) spectra of samples in CDCl_3 were recorded using a Bruker AVANCE II 400 MHz NMR

spectrometer; the internal reference was tetramethylsilane. Two-dimensional ^1H - ^{13}C heteronuclear multiple quantum coherence (HMQC) was measured using the same NMR spectrometer. Fourier transform infrared (FTIR) spectra were recorded using a Nicolet Nexus 670 spectrophotometer. Elemental analysis of the benzoxazine monomer was performed using an elementary analyzer (Elementar Vario EL-III). The molecular weight and polydispersity index (PDI) of the benzoxazine copolymer were measured using gel permeation chromatography (GPC), with tetrahydrofuran (THF) as the solvent and polystyrene (PS) as the standard, at a flow rate of 1 mL min^{-1} . Differential scanning calorimetry (DSC) was performed using a NETZSCH DSC apparatus (model 204f1). The temperature ramp rate was $10 \text{ }^\circ\text{C min}^{-1}$ under a N_2 atmosphere. Dynamic mechanical analysis (DMA) was conducted using a NETZSCH DMA/242E analyzer operated in tension mode, with an amplitude of $10 \text{ }\mu\text{m}$, a temperature ramp rate of $3 \text{ }^\circ\text{C min}^{-1}$, and a frequency of 1 Hz . Thermogravimetric analysis (TGA) was performed using a NETZSCH STA449-C apparatus, from 25 to $850 \text{ }^\circ\text{C}$ at a heating rate of $10 \text{ }^\circ\text{C min}^{-1}$ under N_2 or air. The microstructures of char residues of thermosets after TGA measurements were determined using scanning electron microscopy (SEM); images were collected using a JEOL JSM 6700F microscope operated at 200 kV . The specific heat release rate (HRR, W g^{-1}) and the total heat release (THR, kJ g^{-1}) were recorded using a microscale combustion calorimeter (MCC; Fire Testing Technology), based on the ASTM 7309-2007a standard. The MCC thermogram was recorded from 100 to $750 \text{ }^\circ\text{C}$ at a heating rate of $1 \text{ }^\circ\text{C s}^{-1}$, under a stream of N_2 (80 mL min^{-1}); a stream of O_2 (20 mL min^{-1}) was mixed into the anaerobic thermal degradation products under the N_2 gas stream prior to entering the combustion furnace. The temperature of the combustion furnace was $900 \text{ }^\circ\text{C}$. The dielectric constants and dielectric losses of the polybenzoxazines were recorded at room temperature using a Concept 80 broadband dielectric spectrometer. Prior to dielectric measurements, the films (thickness: $1\text{--}2 \text{ mm}$; diameter: 20 mm) were dried at $100 \text{ }^\circ\text{C}$ for 8 h under vacuum. These sample films were placed between two Cu electrodes to form parallel plate capacitors for dielectric testing.

Bisbenzoxazine monomer with *ortho*-norbornene functionality (*o*HPNI-*oda*)

Xylenes (80 mL), 4,4'-oxydianiline (4.01 g , 0.0200 mol), paraformaldehyde (2.41 g , 0.0800 mol), and *o*HPNI (10.2 g , 0.0400 mol) were mixed in a 500 mL round-bottom flask equipped with a reflux condenser. The mixture was heated under reflux for 24 h and then cooled to room temperature. The reaction product was precipitated into hexanes (100 mL). The crude product was obtained after evaporation of the solvent under vacuum. Recrystallization from toluene/acetone ($1:1$) gave the product (yield *ca.* 87%). IR spectra (KBr), cm^{-1} : 1776 , 1713 (imide I), 1485 (trisubstituted aromatic ring), 1382 (imide II), 1235 (C–O), 927 (oxazine ring), and 697 ($=\text{C}\text{--}\text{H}$). ^1H NMR (CDCl_3), ppm: $\delta = 1.62$ (dt, 2H), 1.80 (dt, 2H), 3.43 (m, 4H), 3.51 (m, 4H), 4.58 (s, 4H, ArCH_2N , oxazine), 5.28 (s, 4H,

OCH₂N, oxazine), 6.23, and 6.28 (dt, 4H), 6.78–7.30 (m, Ar, 14H). Anal. Calcd for C₂₃H₂₀N₂O₃: C, 72.81; H, 5.05; N, 7.38. Found: C, 72.62%; H, 5.10%; N, 7.29%.

Main chain-type poly(benzoxazine-co-imide-co-siloxane) (*o*HPNI-oda-PDMS)

*o*HPNI-oda (2.00 g, 2.64 mmol) and PDMS (1.53 g, 2.64 mmol) were dissolved in toluene (75 mL) in a three-neck flask equipped with a reflux condenser. The mixture was stirred at room temperature under N₂ for 15 min. Pt(dvs) (0.03 wt%, 6 drops) was added into the flask and then the solution was heated at 90 °C. After approximately 48 h, the best conversion to the main chain-type benzoxazine copolymer had occurred, based on the evidence from the ¹H NMR spectra. The solution was cooled to room temperature and washed three times with deionized H₂O. The solution was concentrated through vacuum distillation to obtain a solid product, which was dried in a vacuum oven at 50 °C for 24 h to give the benzoxazine copolymer.

Polymerization of the benzoxazine monomer and copolymer

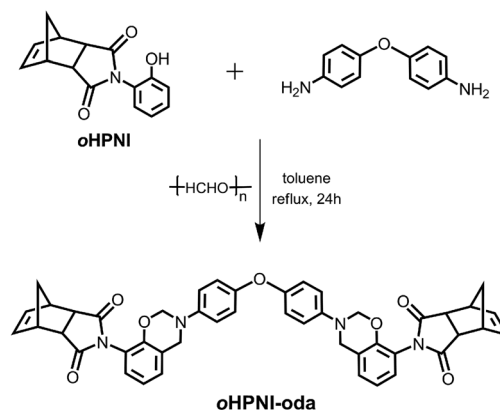
Solutions with 30% solid contents of *o*HPNI-oda and *o*HPNI-oda-PDMS in DMF were prepared. Each solution was cast on a steel mold. The thin films were gradually dried in an air-circulating oven at 120 °C for 48 h to remove the residual DMF solvent. The *o*HPNI-oda and *o*HPNI-oda-PDMS thin films were coated on a glass plate and subjected to stepwise thermal polymerization at 140, 160, 180, 200, 220, and 240 °C for 1 h each to give poly(*o*HPNI-oda) and poly(*o*HPNI-oda-PDMS).

Results and discussion

Synthesis of the bisbenzoxazine monomer and main chain-type poly(benzoxazine-co-imide-siloxane)

The *ortho*-norbornene-functionalized bisbenzoxazine monomer *o*HPNI-oda was prepared through a modified Mannich condensation from an *ortho*-norbornene-functionalized phenol unit (*o*HPNI), a primary diamine (oda), and paraformaldehyde, as displayed in Scheme 2.

The chemical structure of *o*HPNI-oda was characterized using NMR spectroscopy (Fig. 1). The characteristic resonances in the ¹H NMR spectrum of *o*HPNI-oda [Fig. 1(a)], assigned to the ArCH₂N and OCH₂N units of the oxazine rings in the benzoxazine structure, appeared as signals at 4.58 and 5.58 ppm, respectively. The signals of the protons of the olefinic group of the norbornene units appeared at 6.23 and 6.28 ppm. Furthermore, the presence of the norbornene units was confirmed by resonances located in the range 3.52–1.62 ppm. The presence of the norbornene units and the oxazine rings in *o*HPNI-oda was confirmed in the ¹³C NMR spectrum shown in Fig. 1(b). The signals near 51.6 and 80.0 ppm represent the characteristic carbon resonances of the ArCH₂N and OCH₂N units, respectively, in the oxazine rings. In addition, a signal for the typical resonance of a vinylene unit in a norbornene appeared at 134.8 ppm. These assignments for the ¹H and ¹³C



Scheme 2 Synthesis of *o*-norbornene-bisfunctionalized benzoxazine monomer.

NMR signals of the norbornene functionality and the oxazine ring in *o*HPNI-oda were confirmed using two-dimensional (2D) ¹H–¹³C HMQC NMR spectroscopy [Fig. 1(c)].

*o*HPNI-oda contains terminal vinylene units in the norbornene end-caps; we expected them to yield copolymers through hydrosilylation with hydride-terminated PDMS (Scheme 3). The Pt-catalyzed hydrosilylation between *o*HPNI-oda and PDMS was complete within 48 h in toluene under reflux. After the disappearance of the characteristic signals of the protons of the vinylene units (Fig. S1†), the new copolymer *o*HPNI-oda-PDMS was obtained. The apparent molecular weight ($M_n = 3200$) and PDI (1.40) of *o*HPNI-oda-PDMS were obtained through GPC analysis. The molecular weight of this copolymer is rather low when considering the molecular weight of its oligomeric precursor.

The low molecular weight of *o*HPNI-oda-PDMS, with three or four repeating units, was presumably caused by the limited mobility of the polymer chains (induced by the increase in molecular weight), which decreased the accessibility of the terminal units.

The structure of *o*HPNI-oda-PDMS was confirmed from its ¹H NMR spectrum (Fig. 2). The presence of oxazine rings in the newly synthesized copolymer was evidenced by two characteristic signals at 4.65 ppm (ArCH₂N) and 5.30 ppm (OCH₂N) for the methylene units of oxazine rings. Normally, the ¹H NMR spectrum of a benzoxazine monomer would feature two equal-intensity singlets representing the methylene protons in the oxazine ring.⁹ These proton signals would, however, be expected to broaden in the spectrum of such a main chain-type polybenzoxazine copolymer, because of the low chain mobility. The degree of ring closure was approximately 75%, as measured from the integral ratio of the signals for the ring-opened methylene unit (4.70 ppm) and the oxazine-ring methylene unit (5.30 ppm). The ring-opened structures in the polymer backbone could not contribute actively to the thermally activated ring-opening polymerization, but they could still be incorporated into the cross-linked networks in the polybenzoxazine through covalent bonding to a reaction partner or through hydrogen bonding.

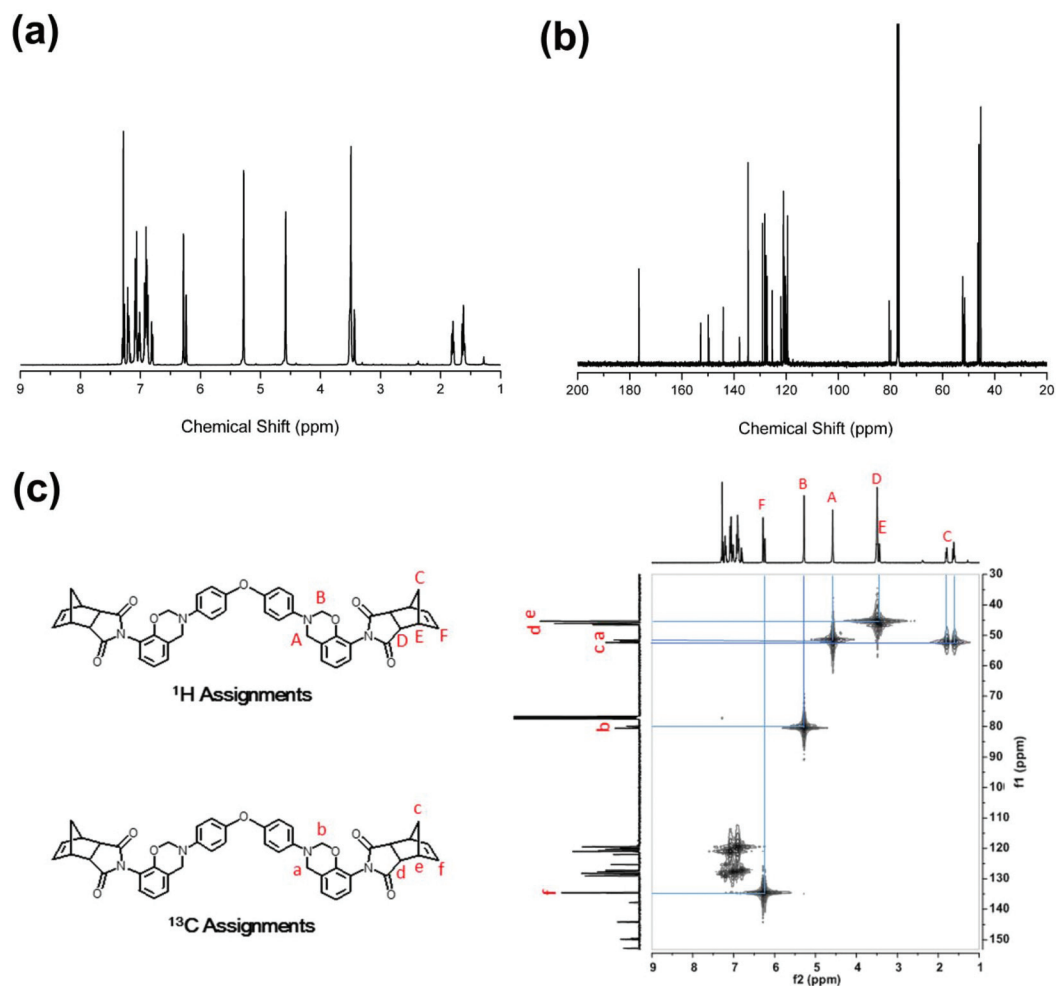
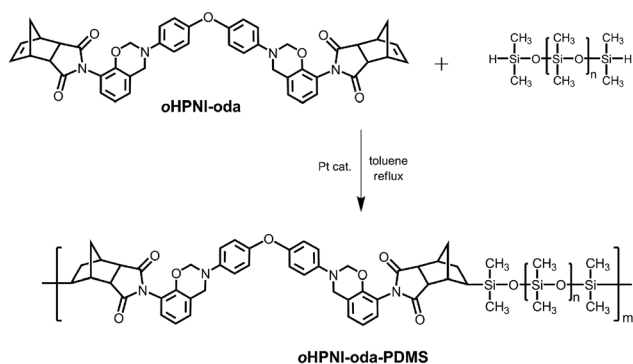


Fig. 1 (a) ^1H and (b) ^{13}C NMR spectra of *o*HPNI-oda. (c) ^1H and ^{13}C NMR signal assignments for *o*HPNI-oda, based on ^1H - ^{13}C HMQC NMR spectroscopy.



Scheme 3 Preparation of *o*HPNI-oda-PDMS.

We recorded FTIR spectra to confirm the chemical structures of *o*HPNI-oda and *o*HPNI-oda-PDMS. Fig. 3 presents, with blue labels, the characteristic bands that verified the presence of various functionalities in our target benzoxazine monomer and copolymer. For instance, the imide groups in *o*HPNI-oda and *o*HPNI-oda-PDMS are represented by bands at

1776, 1713, and 1382 cm^{-1} and at 1774, 1714, and 1381 cm^{-1} , respectively. The doublets in the range from 1710 to 1780 cm^{-1} are assigned to asymmetric imide C-C(=O)-C stretching, while the bands near 1380 cm^{-1} are attributed to the axial stretching of C-N bonds.^{31,32} Furthermore, the presence of aromatic ether units in the benzoxazine rings of *o*HPNI-oda and *o*HPNI-oda-PDMS was confirmed by bands centered at 1235 and 1234 cm^{-1} , respectively, representing C-O-C antisymmetric stretching.³³ In addition, the existence of siloxane groups in *o*HPNI-oda-PDMS was supported by a characteristic band at 2137 cm^{-1} (Si-H stretching) and a strong absorption band at 1093 cm^{-1} (Si-O-Si stretching).²⁰ Moreover, the bands at 927 and 920 cm^{-1} in the spectra of *o*HPNI-oda and *o*HPNI-oda-PDMS, respectively, were mainly related to the presence of their oxazine rings.³⁴

Thermally activated polymerization of benzoxazine units

Fig. 4 reveals the polymerization behavior of both *o*HPNI-oda and *o*HPNI-oda-PDMS, as investigated using DSC. The trace for *o*HPNI-oda exhibited an endotherm at $216\text{ }^\circ\text{C}$, representing the melting behavior, and an exotherm maximum at $259\text{ }^\circ\text{C}$,

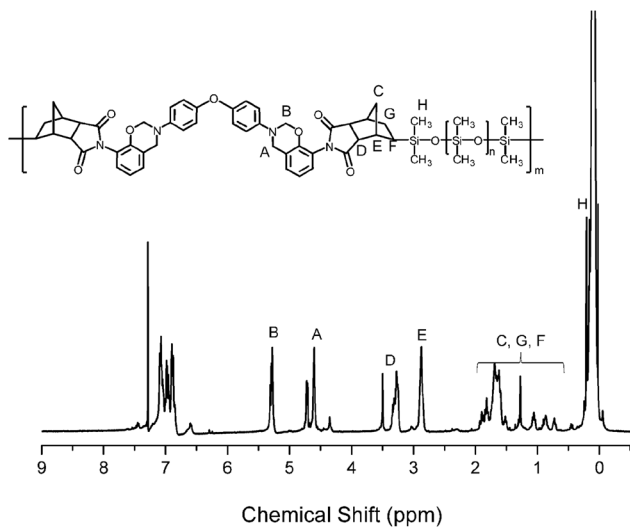


Fig. 2 ^1H NMR spectrum of *o*HPNI-oda-PDMS.

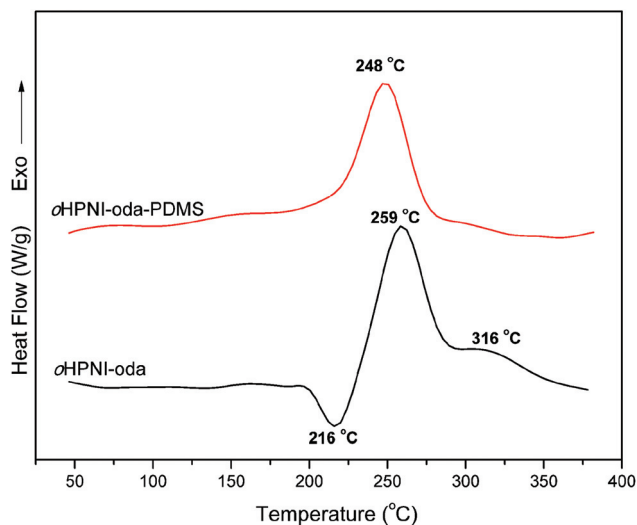


Fig. 4 DSC thermograms of the benzoxazine monomer *o*HPNI-oda and the copolymer *o*HPNI-oda-PDMS.

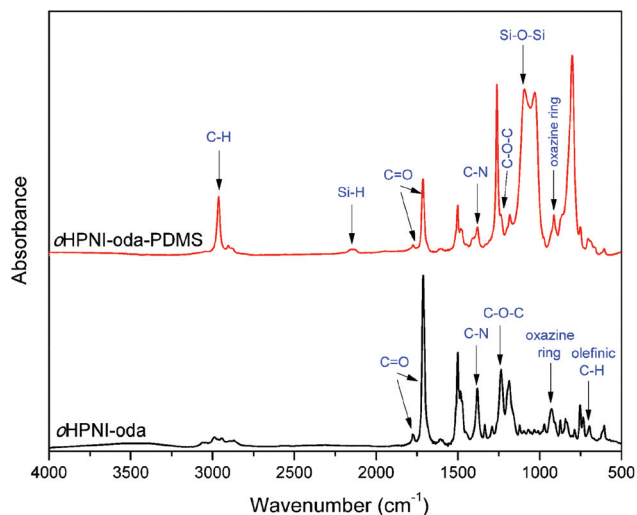


Fig. 3 FTIR spectra of *o*HPNI-oda and *o*HPNI-oda-PDMS.

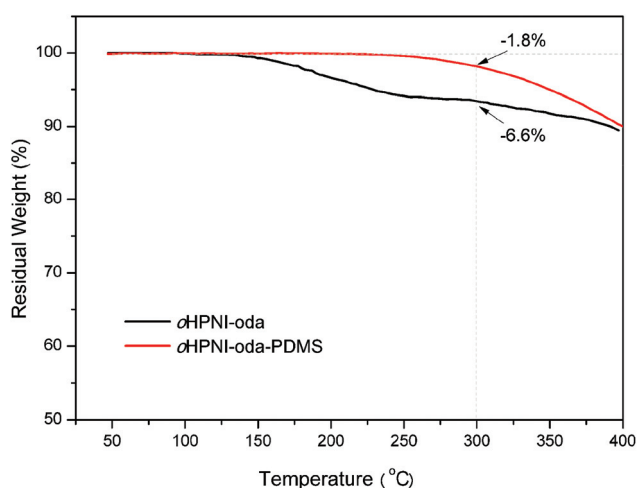


Fig. 5 TGA analysis of the benzoxazine monomer and copolymer.

representing its polymerization. The high rigidity of the norbornene-functionalized bisbenzoxazine resulted in the high melting temperature of *o*HPNI-oda. Another exothermic reaction, with a maximum at 316 °C, was also evident for *o*HPNI-oda. We attribute this second exothermic peak to the polymerization of the nadic end cap, as has been reported for other norbornene-functionalized benzoxazines.²⁷ In contrast, the exotherm maximum for the ring-opening polymerization of *o*HPNI-oda-PDMS had shifted to a relatively lower temperature of 248 °C. We suspect that ring-opened structures formed from *o*HPNI-oda-PDMS acted as efficient initiators for the ring-opening polymerization of the oxazine rings.³⁵

Fig. 5 presents the TGA thermograms of the uncured benzoxazine monomer *o*HPNI-oda and the copolymer *o*HPNI-oda-PDMS. A weight loss of 6.6% occurred during the thermal treatment of *o*HPNI-oda up to 300 °C. This value derived from

the weight loss of *o*HPNI-oda is close to those reported for other difunctionalized benzoxazines.^{36,37} The cleavage of the very unstable zwitterionic intermediate, including *N*-methyleylaniline and phenolic species, significantly increases the weight loss during the ring-opening polymerization of oxazine rings.³⁶ We found, however, that the weight loss during the thermal treatment of *o*HPNI-oda-PDMS up to 300 °C was much lower than that of *o*HPNI-oda. In general, polybenzoxazines derived from monomeric benzoxazines possess more defects at their chain ends, due to the termination of chain propagation of the intramolecular six-membered ring stabilized through hydrogen bonding.^{38,39} The main chain-type benzoxazines with relatively higher molecular weights can minimize the formation of unwanted defects from the terminal chain units, leading to higher thermal stability, relative to that of monomeric benzoxazines, during polymerization.

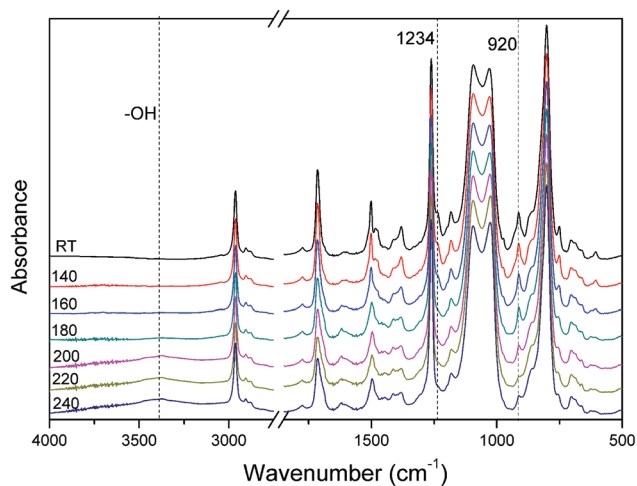
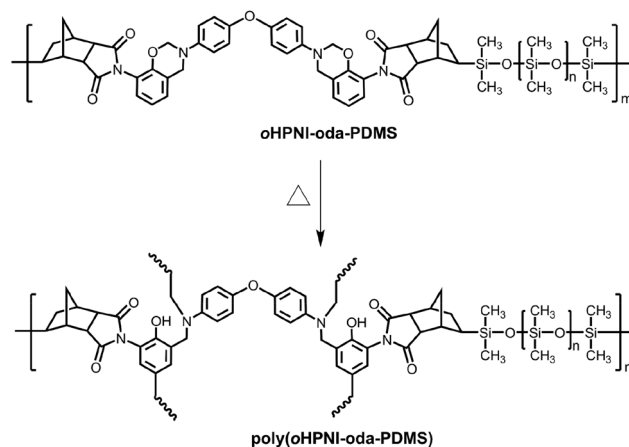


Fig. 6 FTIR spectra of *o*HPNI-oda-PDMS after various thermal treatments.

We used FTIR spectroscopic analyses to further qualitatively study the structural evolution of *o*HPNI-oda and *o*HPNI-oda-PDMS during heating. As displayed in Fig. S2,[†] the intensities of the typical absorption bands at 927 (benzoxazine) and 1235 (C–O–C) cm^{-1} gradually decreased upon increasing the temperature. In addition, the signals for the =C–H units ($>3000 \text{ cm}^{-1}$), due to the nadic rings, and the olefinic C=C units at 697 cm^{-1} decreased in intensity significantly upon heating from 240 to $300 \text{ }^\circ\text{C}$,⁴⁰ indicating that the nadic end caps in *o*HPNI-oda underwent olefinic polymerization of the C=C bonds after the polymerization of the oxazine rings (Fig. S3[†]). Because hydrosilylation had occurred between the vinylene units in the norbornene end groups of *o*HPNI-oda and PDMS, a higher temperature was not required to complete the polymerization, due to the absence of vinylene groups in *o*HPNI-oda-PDMS. Fig. 6 displays the *in situ* FTIR spectra of *o*HPNI-oda-PDMS; the bands at 920 (benzoxazine ring) and $1234 \text{ (C–O–C)} \text{ cm}^{-1}$ gradually disappeared upon increasing the temperature. At the same time, a broad band around 3400 cm^{-1} , which we attribute to strongly overlapping signals for intramolecular $\text{OH}\cdots\pi$, intermolecular $\text{OH}\cdots\text{O}$, and intramolecular $\text{OH}\cdots\text{N}$ hydrogen bonding,⁴¹ gradually emerged upon increasing the temperature. Scheme 4 depicts the structural transformation of *o*HPNI-oda-PDMS during its thermal treatment.

We also used DSC to investigate the thermally activated polymerization behavior of this main chain-type *o*HPNI-oda-PDMS after various thermal treatments. Fig. 7 displays the DSC thermograms of *o*HPNI-oda-PDMS after thermal treatment at various temperatures for 1 h each. The exothermic peak gradually decreased in intensity after the thermal treatment at each temperature, and completely disappeared after heating at $240 \text{ }^\circ\text{C}$, indicating the completion of the thermal polymerization. We also examined the flexibility of *o*HPNI-oda-PDMS. The photograph in the inset to Fig. 7 reveals that *o*HPNI-oda-PDMS was completely flexible after thermal treat-



Scheme 4 Thermally activated ring-opening polymerization of *o*HPNI-oda-PDMS.

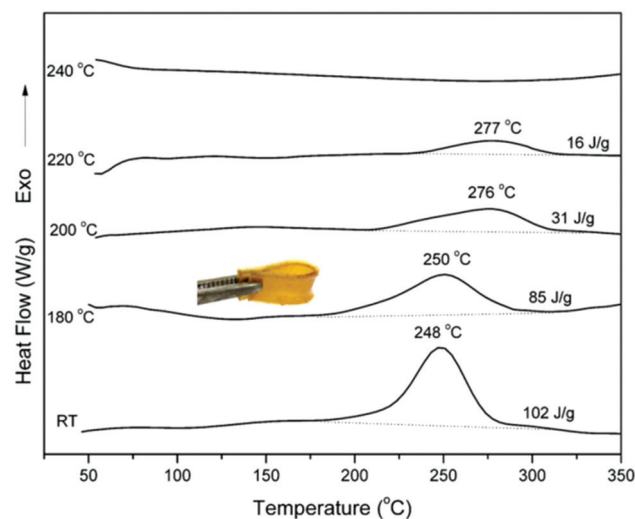


Fig. 7 DSC thermograms of *o*HPNI-oda-PDMS after various thermal treatments; inset: photograph of the slightly polymerized *o*HPNI-oda-PDMS.

ment at $180 \text{ }^\circ\text{C}$ for 1 h. Although the further polymerization of *o*HPNI-oda-PDMS at elevated temperatures decreased the flexibility of the films, the shapes and sizes of these films were retained.

Thermal and heat release properties of polybenzoxazines

We used DMA to investigate the thermomechanical properties of both our thermosets. Fig. S4[†] reveals that the storage modulus of poly(*o*HPNI-oda) maintained a stable value during heating in the initial temperature range, but began decreasing during the glass transition region. In contrast, the modulus increased at the rubbery plateau, as also evidenced in Fig. S4,[†] suggesting a restriction in chain mobility. This behavior was caused by the additional polymerization of the norbornene units, resulting in a further increase in the rigidity of the thermosets. The values of $\tan \delta$ of poly(*o*HPNI-oda) revealed the

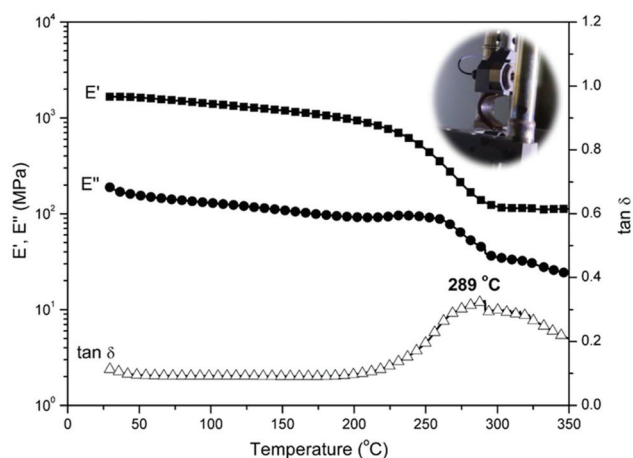


Fig. 8 DMA profile of poly(oHPNI-oda-PDMS); inset: photograph of the film of poly(oHPNI-oda-PDMS) after the DMA measurement.

relaxation phenomenon at 250 °C and an additional less-defined peak at 365 °C, clearly indicating the further polymerization of the norbornene functionalities and the formation of a rigid cross-linked network with lower segmental mobility. Fig. 8 presents the DMA profile of poly(oHPNI-oda-PDMS). As seen from Fig. 8, the value of T_g , assigned as the peak temperature from the $\tan \delta$ curve, was as high as 289 °C. Although additional cross-linking from the norbornene groups could not occur, the value of T_g of poly(oHPNI-oda-PDMS) was relatively much higher than those of other reported main chain-type polybenzoxazines.^{14,18,42} Moreover, the film of poly(oHPNI-oda-PDMS) maintained some flexibility after the DMA measurement, as indicated in the inset to Fig. 8.

We also investigated the thermal stabilities of poly(oHPNI-oda) and poly(oHPNI-oda-PDMS) through TGA analyses under both N_2 and air atmospheres. For poly(oHPNI-oda) (Fig. 9), the first weight-loss stage from 350 to 550 °C, under both N_2 and air, was presumably due to the partial decomposition of the terminal defect structures of the polybenzoxazine.⁴³

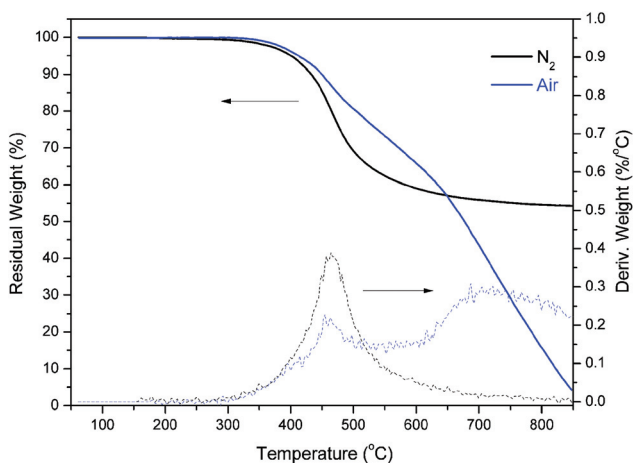


Fig. 9 TGA traces of poly(oHPNI-oda) under both N_2 and air.

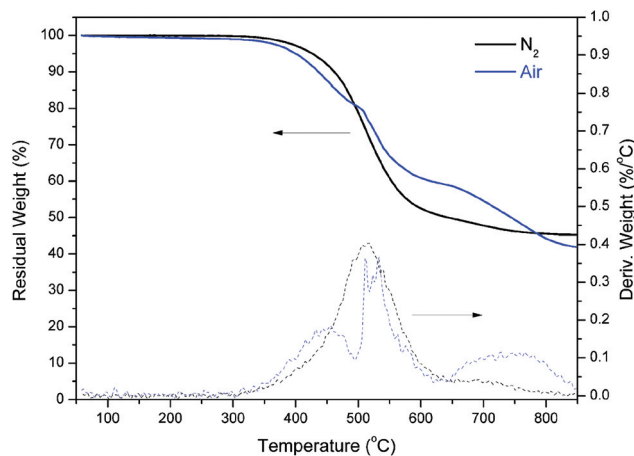


Fig. 10 TGA analyses of poly(oHPNI-oda-PDMS) under both N_2 and air.

Poly(oHPNI-oda) exhibited excellent thermal stability, with values of T_{d5} of 400 (N_2) and 412 (air) °C and values of T_{d10} of 431 (N_2) and 449 (air) °C. The improved thermal stability of poly(oHPNI-oda) during the initial degradation stage under air was possibly due to the oxidation of methylene-containing linkages in the polybenzoxazine network.

In contrast, poly(oHPNI-oda-PDMS) exhibited obviously different degradation behavior under N_2 and air. Fig. 10 reveals that poly(oHPNI-oda-PDMS) provided a single modal degradation profile, where the maximum weight-loss rate occurred at 513 °C under the N_2 atmosphere, whereas it exhibited a multi-modal degradation profile under air. Poly(oHPNI-oda-PDMS) also exhibited very good thermal stability, with values of T_{d5} of 429 (N_2) and 400 (air) °C and values of T_{d10} of 461 (N_2) and 436 (air) °C. In contrast to the behavior of poly(oHPNI-oda), poly(oHPNI-oda-PDMS) possessed higher thermal stability under N_2 than under air, presumably because of the presence of less thermally stable segments of PDMS in poly(oHPNI-oda-PDMS). The methyl groups of the PDMS units in poly(oHPNI-oda-PDMS) would presumably readily degrade during the initial degradation stage under air. In addition, poly(oHPNI-oda-PDMS) provided very similar char yields under both N_2 (46%) and air (45%). We used SEM to study the morphologies and elemental compositions of the char residues from poly(oHPNI-oda-PDMS) after TGA treatment under both N_2 and air (Fig. 11). The Si mappings in Fig. 11b and e indicate that inorganic silicides were dispersed homogeneously on the surfaces of both the residues. Moreover, the results from EDS spectroscopy in Fig. 11c and f indicate that a silica layer was formed in the char residue of poly(oHPNI-oda-PDMS) only after TGA treatment in air, whereas both silica and carbon residues were formed under N_2 . The inorganic layer formed during thermal treatment could protect the underlying polymers by limiting heat.

We used MCC analysis to measure the flammability of the thermosets derived from the benzoxazine monomer and the copolymer. Here, heat release is quantified by the standard O_2 consumption,⁴⁴ with the heat release rate (HRR) given by divid-

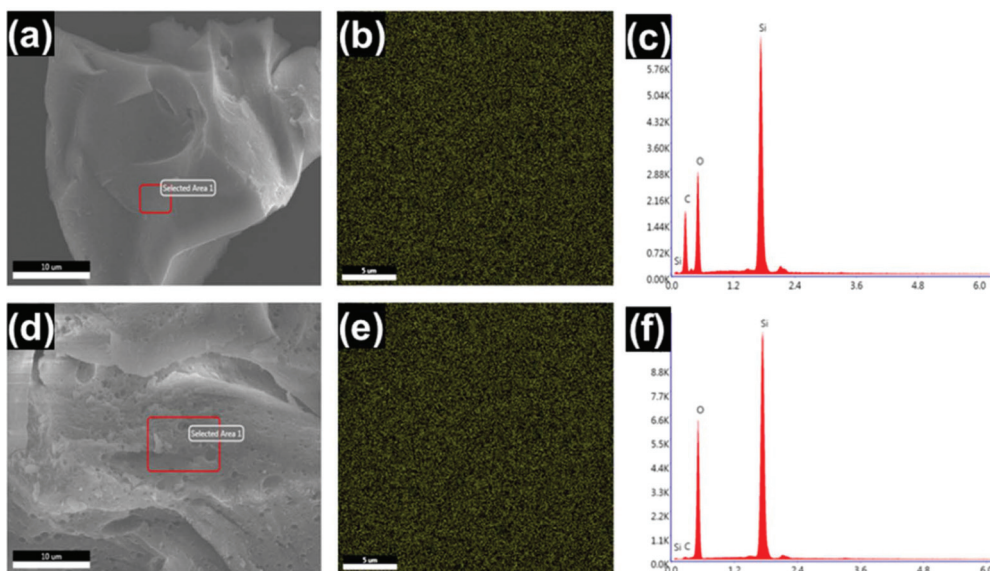


Fig. 11 (a, d) SEM images, (b, e) Si-mappings, and (c, f) EDS analyses of the char residues of poly(*o*HPNI-*oda*-PDMS) after TGA treatment under (a–c) N_2 and (d–f) air.

ing dQ/dt for the initial sample mass at each time interval. In addition, the heat release capacity (HRC) is provided by dividing the maximum HRR by the heating rate.

We performed the MCC analyses of poly(*o*HPNI-*oda*) and poly(*o*HPNI-*oda*-PDMS) from 100 to 750 °C with the heating rate of 1 °C s^{-1} (Fig. 12a), giving HRCs of 150.6 and 80.5 $J g^{-1} K^{-1}$, respectively. In addition, poly(*o*HPNI-*oda*) and poly(*o*HPNI-*oda*-PDMS) provided THRs of 13.5 and 12.7 $kJ g^{-1}$, as revealed in Fig. 12b. Lower values of HRC and THR correspond to a material displaying higher performance in terms of flame resistance. An HRC of less than 300 $J g^{-1} K^{-1}$ can be considered as self-extinguishing, whereas a material with a value of less than 100 $J g^{-1} K^{-1}$ can be considered non-ignitable.⁴⁵ Clearly, the introduction of PDMS units in the cross-linking network provided a substantial decrease in the HRC. As a result, this poly(benzoxazine-*co*-siloxane) copolymer would appear to have potential applications as a low-flammability material.

Dielectric properties of polybenzoxazines

We measured the dielectric properties of poly(*o*HPNI-*oda*) and poly(*o*HPNI-*oda*-PDMS) at room temperature upon varying the frequency of the applied field. As displayed in Fig. 13, the dielectric constants for both polybenzoxazines decreased slightly upon increasing the frequency. For example, the dielectric constant decreased from 2.64 to 2.58 for poly(*o*HPNI-*oda*) within the frequency range from 1 Hz to 1 MHz. Furthermore, poly(*o*HPNI-*oda*-PDMS) exhibited relatively lower dielectric constants, varying from 2.36 to 2.29, in the same frequency range. In general, the dielectric constants of traditional benzoxazine resins fall in the range from approximately 3.0 to 3.5 at 1 MHz, slightly greater than the values measured from low-dielectric-constant materials ($k < 3.0$).^{46,47} As expected, the polybenzoxazine derived from our newly synthesized *ortho*-nor-

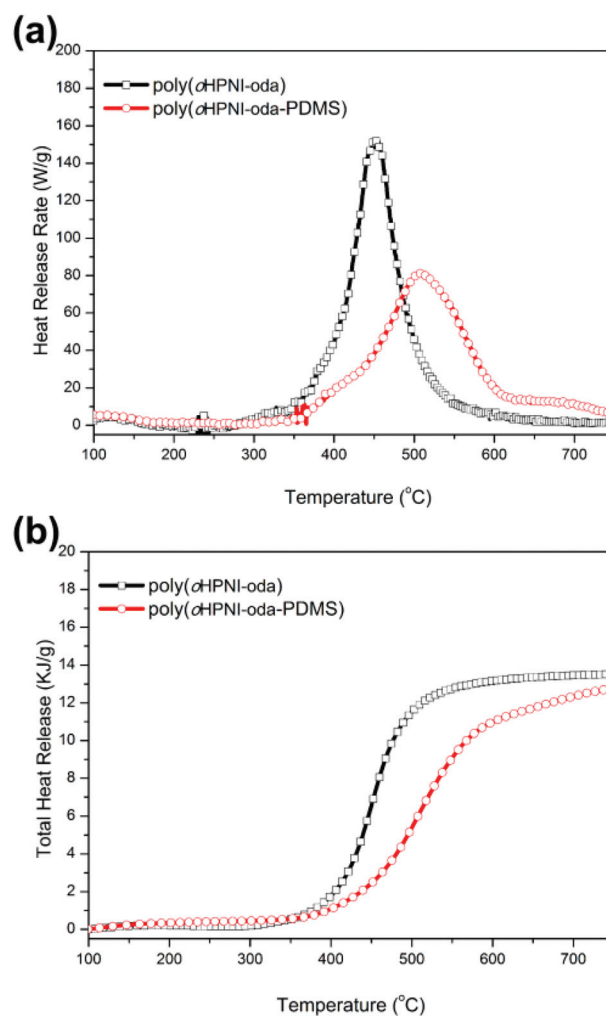


Fig. 12 (a) HRR and (b) THR plotted with respect to temperature for poly(*o*HPNI-*oda*) and poly(*o*HPNI-*oda*-PDMS).

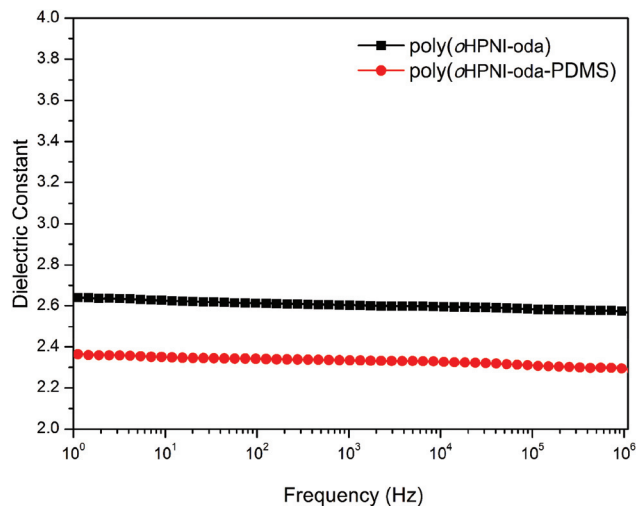


Fig. 13 Dielectric constants plotted with respect to frequency for poly(oHPNI-oda) and poly(oHPNI-oda-PDMS), measured at room temperature.

bornene-bisfunctionalized benzoxazine monomer possessed a low dielectric constant, close to the values previously reported for another norbornene-functionalized benzoxazine resin.²⁸ Notably, the low dielectric constants of poly(oHPNI-oda-PDMS) are comparable to those of fluorinated polybenzoxazoles (2.19 at 1 MHz).²⁹ Thus, the introduction of PDMS into the benzoxazine resin lowered the dielectric constant significantly relative to that of the corresponding polybenzoxazine. The cross-linked networks formed by connected rigid aromatic and soft PDMS segments might have lowered the dielectric constant by increasing the free volume and decreasing the degree of moisture absorption.

Fig. S5† displays the dependence of the $\tan \delta$ curves of poly(oHPNI-oda) and poly(oHPNI-oda-PDMS) in the frequency range from 1 Hz to 1 MHz. The values of $\tan \delta$ ranged from 0.005 to 0.002 for poly(oHPNI-oda). These values are slightly lower than those from 0.007 to 0.002 obtained for poly(oHPNI-oda-PDMS). Moreover, the dielectric losses for both polybenzoxazines were as low as 0.003 at 1 MHz. Table 1 summarizes the thermal and dielectric properties of poly(oHPNI-oda) and poly(oHPNI-oda-PDMS). The dielectric data suggest that our newly developed polybenzoxazines should be suitable for applications requiring both low values of k and high thermal stability.

Table 1 Thermal stability, heat release, and the dielectric properties of polybenzoxazines

Sample	N ₂		Air		HRC (J g ⁻¹ K ⁻¹)	THR (kJ g ⁻¹)	Dielectric constant (at 1 MHz)
	T _{d5} (°C)	Y _c (%)	T _{d5} (°C)	Y _c (%)			
Poly(oHPNI-oda)	400	55	412	15	150.6	13.5	2.58
Poly(oHPNI-oda-PDMS)	427	46	400	45	80.5	12.7	2.29

Conclusions

A new main chain-type copolymer, poly(benzoxazine-co-imide-co-siloxane), has been synthesized through hydrosilylation of an *ortho*-norbornene-functionalized bisbenzoxazine monomer and PDMS. The resulting polybenzoxazines derived from both the benzoxazine monomer and the copolymer exhibited excellent high thermal stabilities and low dielectric constants. Notably, the main chain-type poly(benzoxazine-co-imide-co-siloxane)-based polybenzoxazine poly(oHPNI-oda-PDMS) displayed high thermal stability with a value of T_g of 289 °C and values of T_{d5} of greater than 400 °C under both N₂ and air. In addition, poly(oHPNI-oda-PDMS) exhibited low flammability, with a low HRC (80.5 J g⁻¹ K⁻¹) as well as a low THR (12.7 kJ g⁻¹). Moreover, poly(oHPNI-oda-PDMS) possessed very low dielectric constants (2.36–2.29) over the frequency range from 1 Hz to 1 MHz.

Conflicts of interest

There are no conflicts to declare.

Acknowledgements

The financial support from the National Natural Science Foundation of China (no. 51603093), the Science and Technology Agency of Jiangsu Province (no. BK 20160515) and the China Postdoctoral Science Foundation (no. 2016M600369 and 2018T110451) is gratefully acknowledged.

Notes and references

- 1 A. F. M. El-Mahdy and S. W. Kuo, *Polym. Chem.*, 2018, **9**, 1815–1826.
- 2 C. Zúñiga, L. Bonnaud, G. Lligadas, J. C. Ronda, M. Galià, V. Cádiz and P. Dubois, *J. Mater. Chem. A*, 2014, **2**, 6814–6822.
- 3 H. J. Kim, Z. Brunovska and H. Ishida, *Polymer*, 1999, **40**, 6565–6573.
- 4 C. Sutapin, N. Mantaranon and S. Chirachanchai, *J. Mater. Chem. C*, 2017, **5**, 8288–8294.
- 5 H. Ishida and D. J. Allen, *J. Polym. Sci., Part B: Polym. Phys.*, 1996, **34**, 1019–1030.
- 6 J. Y. Wu, M. G. Mohamed and S. W. Kuo, *Polym. Chem.*, 2017, **8**, 5481–5489.
- 7 Y. X. Wang and H. Ishida, *Polymer*, 1999, **40**, 4563–4570.
- 8 A. Sudo, L. C. Du, S. Hirayama and T. Endo, *J. Polym. Sci., Part A: Polym. Chem.*, 2010, **48**, 2777–2782.
- 9 H. Ishida and T. Agag, *Handbook of Benzoxazine Resins*, Elsevier, Amsterdam, 2011.
- 10 H. Ishida and P. Froimowicz, *Advanced and Emerging Polybenzoxazine Science and Technology*, Elsevier, Amsterdam, 2017.

- 11 B. Kiskan and Y. Yagci, Benzoxazine resins as smart materials and future perspectives, in *Thermosets*, Elsevier, 2018, pp. 543–576.
- 12 B. Kiskan, *React. Funct. Polym.*, 2018, **129**, 76–78.
- 13 X. Ning and H. Ishida, *J. Polym. Sci., Part A: Polym. Chem.*, 1994, **32**, 1121–1129.
- 14 T. Takeichi, T. Kano and T. Agag, *Polymer*, 2005, **46**, 12172–12180.
- 15 A. Chernykh, J. Liu and H. Ishida, *Polymer*, 2006, **47**, 7664–7669.
- 16 T. Agag and T. J. Takeichi, *Polym. Sci., Part A: Polym. Chem.*, 2007, **45**, 1878–1888.
- 17 B. Kiskan, G. Demiray and Y. Yagci, *J. Polym. Sci., Part A: Polym. Chem.*, 2008, **46**, 3512–3518.
- 18 M. Zeng, J. Chen, Q. Xu, Y. Huang, Z. Feng and Y. Gu, *Polym. Chem.*, 2018, **9**, 2913–2925.
- 19 K. D. Demir, B. Kiskan, S. S. Latthe, A. L. Demirel and Y. Yagci, *Polym. Chem.*, 2013, **4**, 2106–2114.
- 20 Y. T. Liao, Y. C. Lin and S. W. Kuo, *Macromolecules*, 2017, **50**, 5739–5747.
- 21 B. Kiskan, B. Aydogan and Y. Yagci, *J. Polym. Sci., Part A: Polym. Chem.*, 2009, **47**, 804–811.
- 22 K. C. Chen, H. T. Li, W. B. Chen, C. H. Liao, K. W. Sun and F. C. Chang, *Polym. Int.*, 2011, **60**, 436–442.
- 23 K. C. Chen, H. T. Li, S. C. Huang, W. B. Chen, K. W. Sun and F. C. Chang, *Polym. Int.*, 2011, **60**, 1089–1096.
- 24 W. C. Chen and S. W. Kuo, *Macromolecules*, 2018, **51**, 9602–9612.
- 25 J. Liu and H. Ishida, *Macromolecules*, 2014, **47**, 5682–5690.
- 26 K. Zhang, J. Liu, S. Ohashi, X. Liu, Z. Han and H. Ishida, *J. Polym. Sci., Part A: Polym. Chem.*, 2015, **53**, 1330–1338.
- 27 K. Zhang and H. Ishida, *Polymer*, 2015, **66**, 240–248.
- 28 K. Zhang and X. Yu, *Macromolecules*, 2018, **51**, 6524–6533.
- 29 K. Zhang, L. Han, P. Froimowicz and H. Ishida, *Macromolecules*, 2017, **50**, 6552–6560.
- 30 K. Zhang, Z. Shang, C. J. Evans, L. Han, H. Ishida and S. Yang, *Macromolecules*, 2018, **51**, 7574–7585.
- 31 S. T. Wellinghoff, H. Ishida, J. L. Koenig and E. Baer, *Macromolecules*, 1980, **13**, 826–834.
- 32 B. T. Low, Y. Xiao, S. C. Tai and L. Ye, *Macromolecules*, 2008, **41**, 1297–1309.
- 33 J. Dunkers and H. Ishida, *Spectrochim. Acta*, 1995, **51A**, 1061–1074.
- 34 L. Han, D. Iguchi, P. Gil, T. R. Heyl, V. M. Sedwick, C. R. Arza, S. Ohashi, D. J. Lacks and H. Ishida, *J. Phys. Chem. A*, 2017, **121**, 6269–6282.
- 35 S. Ohashi, D. Iguchi, T. R. Heyl, P. Froimowicz and H. Ishida, *Polym. Chem.*, 2018, **9**, 4194–4204.
- 36 N. K. Sini and T. Endo, *Macromolecules*, 2016, **49**, 8466–8478.
- 37 Y. Liu, R. Yin, X. Yu and K. Zhang, *Macromol. Chem. Phys.*, 2019, **220**, 1800291.
- 38 A. Laobuthee, S. Chirachanchai, H. Ishida and K. Tashiro, *J. Am. Chem. Soc.*, 2001, **123**, 9947–9955.
- 39 S. Chirachanchai, A. Laobuthee and S. Phongtamrug, *J. Heterocycl. Chem.*, 2009, **46**, 714–721.
- 40 J. N. Hay, J. D. Boyle, S. F. Parker and D. Wilson, *Polymer*, 1989, **30**, 1032–1040.
- 41 H. D. Kim and H. Ishida, *Macromol. Symp.*, 2003, **195**, 123–140.
- 42 M. Baqar, T. Agag and H. Ishida, *Polymer*, 2011, **52**, 307–317.
- 43 I. Hamerton, S. Thompson, B. J. Howlin and C. A. Stone, *Macromolecules*, 2013, **46**, 7605–7615.
- 44 R. E. Lyon and R. N. Walters, *J. Anal. Appl. Pyrolysis*, 2004, **71**, 27–46.
- 45 R. N. Walters and R. E. Lyon, *J. Appl. Polym. Sci.*, 2003, **87**, 548–563.
- 46 J. Dong, C. Yang, Y. Cheng, T. Wu, X. Zhao and Q. Zhang, *J. Mater. Chem. C*, 2017, **5**, 2818–2825.
- 47 R. Bei, C. Qian, Y. Zhang, Z. Chi, S. Liu, X. Chen, J. Xu and M. P. Aldred, *J. Mater. Chem. C*, 2017, **5**, 12807–12815.